Cogn Comput
DOI 10.1007/s12559-010-9074-z

Clustering of Gaze During Dynamic Scene Viewing is Predicted by Motion

Parag K. Mital · Tim J. Smith · Robin L. Hill · John M. Henderson

Received: 23 April 2010 / Accepted: 5 October 2010

Abstract Where does one attend when viewing dynamic scenes? Research into the factors influencing gaze location during static scene viewing have reported that low-level visual features contribute very little to gaze location especially when opposed by high-level factors such as viewing task. However, the inclusion of transient features such as motion in dynamic scenes may result in a greater influence of visual features on gaze allocation and coordination of gaze across viewers. In the present study, we investigated the contribution of low- to mid-level visual features to gaze location during free-viewing of a large dataset of videos ranging in content and length. Signal detection analysis on visual features and Gaussian Mixture Models for clustering gaze was used to identify the contribution of visual features to gaze location. The results show that mid-level visual features including corners and orientations can distinguish between actual gaze locations and a randomly sampled baseline. However, temporal features such as flicker, motion, and their respective contrasts were the most predictive of gaze location. Additionally, moments in which all viewers' gaze tightly clustered in the same location could be predicted by motion. Motion and mid-level visual features may influence gaze allocation in dynamic scenes, but it is currently unclear whether this influence is involuntary or due to correlations with higher order factors such as scene semantics.

Keywords Eye movements · Dynamic scenes · Features · Visual attention · Clustering

All eye-movement data and visualization tools can be obtained from: http://thediemproject.wordpress.com.

P. K. Mital (✉)
Department of Computing Goldsmiths, University of London, London, UK
e-mail: pkmital@gmail.com

T. J. Smith
Department of Psychological Sciences, Birkbeck, University of London, London, UK

R. L. Hill
Department of Psychology, School of Philosophy, Psychology and Language Sciences, University of Edinburgh, Edinburgh, UK

J. M. Henderson
Department of Psychology and McCausland Center for Brain Imaging, University of South Carolina, Columbia, SC, USA
e-mail: john.henderson@sc.edu

Introduction

Eye movements are a real-time index of visual attention and cognition. Due to processing and visual acuity limitations, our eyes shift (*saccade*) up to five times every second so that the light from the area of the scene we are interested in is projected onto the most sensitive part of the retina (the *fovea*). Perception of visual detail and encoding in memory only occurs for the information at the center of attention when the eyes stabilize on a point in space (*fixations*) [1–3]. The factors that influence how we distribute our attention while viewing static visual arrays and scenes have received a lot of attention (see [3, 4] for reviews), but very little is known about how we attend to more realistic dynamic scenes.

The earliest investigations of eye movement behavior during scene viewing [5, 6] portrayed two main ways in which visual attention can be controlled: involuntary capture of attention by external, stimulus features such as luminance and color (*exogenous*) and voluntary allocation of attention according to internal, cognitive factors that focus attention on cognitively relevant features of the

Published online: 22 October 2010

world (*endogenous*). Being involuntary, exogenous control should be consistent across all viewers leading to a high degree of coordination in where and when multiple viewers attend given the same stimuli. By comparison, endogenous control should result in less coordination of attention across individuals as the internal cognitive states of the individual and their relation to the current stimuli are less predictable. Previous evidence of the contribution of exogenous and endogenous factors to gaze control during scene viewing is mixed. When participants free-view still images presented on a computer screen, low-level image properties in static scenes differ significantly at fixation compared to control locations [7–15]. Specifically, high-spatial frequency edge information is higher at fixation than at control locations [7, 8, 11, 12, 15], as is local contrast (the standard deviation of luminance at fixation) [8, 9, 13–15], texture [16], and mid-level visual features composed of multiple superimposed orientations, including corners [17, 18].

The discovery of distinct visual features around fixation led to the development of several computational models of attentional allocation in scenes e.g. [19–25]. These models are all predicated on the assumption that conspicuous visual features "pop-out" and involuntarily capture attention [26]. This assumption is founded on evidence from classic visual search paradigms using simple visual arrays e.g. [27] which have shown that visual features such as color, motion, and orientation can be used to guide attention (see [4] for review). Computational models of attention allocation combine multiple basic visual features at multiple spatial scales in order to produce a *saliency map*: an image distribution predicting the conspicuity of specific locations and their likelihood of attracting attention [19, 26, 28]. The widely used computational model of visual saliency developed by Itti and Koch [19, 28] has been shown to predict fixation locations better than chance under some conditions [21, 28]. For example, medium salience objects are fixated earlier than low-salience objects during memorization [29]. However, subsequent investigations have shown that the model's predictions are correlational in nature and not causal. Visual saliency correlates with objects [30] and is biased toward the screen center in the same way fixations are [15]. Visual salience explains very little of the variance of fixation locations when this correlation is removed by instructing viewers to search for a particular target [8, 29, 31–34]. The visual features used to compute visual saliency are also used by our early visual system to identify higher order features such as objects which are the intended target of attention [30, 35]. During interactive tasks, endogenous control becomes even more pronounced as gaze is tightly linked to the completion of goals such as steering a car, filling a kettle, or walking down the street [36–39].

However, it could be argued that previous investigations into the relationship between visual saliency and gaze in static scenes have been biased against saliency due to the omission of the visual feature shown to most robustly capture attention: motion. The unexpected onset of a new object and the associated motion transients are the only visual features shown to robustly capture visual attention without endogenous pre-setting (i.e. the instruction to search for a specific feature such as "red") [40–42]. Given that onsets do not normally occur in static scenes, no exogenous control should be predicted. Only with the artificial addition of onsets into a static scene is exogenous control observed resulting in immediate fixation of the new object [43–45]. It is not necessarily the new object that captures attention but the motion transients associated with its appearance (see [46] for review). If an onset occurs during a saccade, saccadic suppression masks the motion transients caused by the object's appearance and no oculomotor capture occurs [43–45]. The sudden appearance of new objects and the associated motion transients are the only visual features that are known to exogenously control attention irrespective of endogenous factors [40], and neither feature occurs in static scenes. However, both occur in abundance in dynamic scenes.

The recent addition of dynamic visual features such as motion and difference-over-time (*flicker*) to computational models of visual saliency has resulted in a significant increase in their ability to predict human gaze location in dynamic scenes compared to models which only utilize static features, e.g. color, intensity, and edges [47–53]. Motion and flicker are the strongest independent predictors of gaze location in dynamic scenes, and their independent contributions are as high, if not higher, than the weighted combination of all features in a model of visual salience [48, 50]. However, most previous investigations of dynamic scene viewing have heavily biased the viewing conditions toward exogenous control. Viewers have been biased toward motion by being instructed to "follow the main actors or actions" [48–51] and by using very short video clips (1–3 s) edited together into an unrelated sequence that minimizes the contribution of endogenous factors such as memory and ongoing event comprehension [48, 49]. Carmi and Itti [48, 49] showed that exogenous control was highest immediately following a cut to a new, semantically unrelated scene and decreased monotonically over the next 2.5 s. Studies that have used longer video sequences have also been potentially confounded by the impact of cuts as the videos used were "found" footage gathered from television, film, or home movies and analysis was performed across the entire video [47, 50–52]. Without isolating cuts, it is unclear whether the contribution of visual features to fixation location is due to exogenous control within an ongoing dynamic event or due to the sudden, abrupt presentation of a new scene following a cut.

As well as, predicting higher visual feature values at fixation compared to control locations, exogenous control

of attention may also predict clustering of the gaze of multiple viewers in the same location. If the contrast between visual features at a specific scene region and the whole scene causes the region to "pop-out", then viewers should be involuntarily drawn to the same location at the same time. This would create a high degree of consistency in where viewers attend in a dynamic scene. Such clustering of gaze during dynamic scene viewing has been reported in several studies [48, 54–62] and is believed to be an integral part of film viewing (see [63] for a review). For example, Goldstein et al. [54] showed 20 adults six long clips from Hollywood movies and found that for more than half of the viewing time the distribution of fixations from all viewers occupied less than 12% of the screen area. This *Attentional Synchrony* effect is observed for feature films [48, 54–58, 60–63], television [59], and videos of real-world scenes [53, 60, 64].

In static scenes, fixations from multiple viewers have been shown to cluster in specific scene regions but not at the same time [12]. The only exception is a bias of fixations toward the screen center [15, 65], which has also been observed in dynamic scenes [52]. A systematic analysis of the factors contributing to this central bias in dynamic scenes suggests that it is due to a bias in positioning focal, foreground objects at screen center and a tendency for viewers to saccade to the screen center immediately following scene onset (or following a cut) [66]. Both of these factors explain why a sudden increase in clustering has been observed immediately following cuts [48, 53]. The central bias also presents problems for analyses of visual features at fixation as saliency has also been shown to have a slight but significant center bias in natural scenes [15, 67]. Therefore, the higher visual features reported at fixation may be an incidental consequence of the tendency to cluster gaze at screen center immediately following cuts. Given confounds of central tendency and cuts in previous studies, it is currently unclear what contribution visual features make to gaze clustering during dynamic scene viewing. The only way to subtract the effect of central tendency from the contribution of visual features to gaze location is to (1) present dynamic scenes for longer to give the eyes time to explore the scene; and (2) compare the visual features at fixation to control locations which share the same central tendency (e.g. fixations sampled from a different time point during the same movie [15, 65]). These methods were adopted in the present study.

The Dynamic Scene Study

What are the contributions of low and mid-level static and dynamic visual features to attention during dynamic scene viewing? Do visual features contribute more when gaze of multiple viewers is tightly clustered and do such moments occur throughout a dynamic event independent of cinematic features such as cuts? The present study investigated these questions by recording the eye movements of 42 adults while they watched 26 high-definition videos ranging in length (27 to 217 s), content, and complexity. A range of low- and mid-level visual features including luminance, colors, edges, corners, orientation, flicker, motion and their respective contrasts, were identified in the videos and signal detection methods were used to identify whether each feature dimension could distinguish between fixated and control locations.

Methodology

Participants

Forty-two participants (17 males, 25 females) were recruited through the University of Edinburgh Student and Graduate Employment Service. Ages ranged from 18 to 36 (mean 23). All provided informed consent, had normal/corrected-to-normal vision, received payment upon completion and were naïve to the underlying purposes of the experiment.

Materials

Dynamic image stimuli comprised 26 movies sourced from publicly accessible repositories covering genres including advertisements, documentaries, game trailers, movie trailers, music videos, news clips and time-lapse footage, ranging from 27 to 217 s in length. All videos were converted from their original sources to a 30 frame-per-second Xvid MPEG-4 video file in an Audio/Video-Interleave (avi) container for a total of 78,167 frames across all movies. Appendix 1 details the movies used along with their native resolutions and durations.

Apparatus and Technical Specifications

Participants' eye movements were monitored binocularly using an SR Research Eyelink 2000 desktop mounted eye tracker sampling at 1,000 Hz for each eye. Videos were displayed in random order in their native resolutions and centered on a 21″ Viewsonic Monitor with desktop resolution 1,280 × 960@120 Hz at a viewing distance of 90 cm. Standard stereo desktop speakers delivered the audio media component. Response choices were recorded via a Microsoft Sidewinder joypad. Presentation was controlled using the SR Research Experiment Builder software.

Procedure

Participants were informed that they would watch a series of short, unconnected video clips. They were told that these

clips would be the kind of things broadcast on television or available over the Internet and that they did not contain anything offensive or shocking. Following each clip, instructions would appear on the screen asking them to rate how much they had liked it on a scale from 1 to 4, by pressing the relevant button on the joypad. This ensured some interactivity without interfering with the free-viewing task. The order of the clips was randomized across participants. The experiment itself took approximately 45 min, resulting in the entire testing process, including set-up, instructions, calibration and debriefing lasting about an hour.

A chin and headrest (unrestrained) was used throughout. A thirteen-point binocular calibration preceded the experiment. Central fixation accuracy was tested prior to each trial, with a full calibration repeated when necessary. The central fixation marker also served as a cue for the participant and offered an optional break-point in the procedure. After checking for a central fixation, the experimenter manually triggered the start of each trial.

Eye Movement Parsing

In order to identify where participants were attending while watching the films, a novel method for parsing the raw gaze data was required. Traditional eye movement parsing algorithms implemented in all commercial eye tracking systems assume a fixation and saccade sequence broken up by the occasional blink. This assumption is valid for static stimuli presented at a fixed depth. However, when the stimuli move relative to the participant or the participant relative to the stimuli, other ocular events occur that must be accommodated in the analysis. Smooth pursuit eye movements occur when the eyes pursue an object moving at a low velocity (<100°/s) relative to the head [68]. Initiation of smooth pursuit is generally only possible in the presence of a moving target as a visual signal is required to calibrate the vector of the eye motion [68]. During pursuit, the eyes stabilize the image of the pursued object on the retina allowing visual processing of the pursued object to occur while the image of the periphery is smeared across the retina [69]. If the entire visual field moves relative to the head (e.g. during a camera pan), the eye will exhibit optokinetic nystagmus. Optokinetic nystagmus is a cycle of smooth pursuits in one direction followed by saccades back in the other direction [68]. The velocity range of pursuit eye movements during both smooth pursuit and optokinetic nystagmus overlaps with that of saccadic eye movements leading to misclassification by traditional parsing algorithms. In order to account for the displacement caused by the smooth pursuit movement, traditional parsing of eye movements divide periods of pursuit into a sequence of long phantom fixations joined by phantom saccades. Because the eyes are assumed to be stationary during a fixation, the location of the phantom fixations is taken as the average *X*/*Y* coordinates of the eyes during the pursuit movement. This creates a sequence of fixations that are either ahead of or behind the actual gaze location and the object being pursued.

As we were interested in the visual features at the center of gaze during dynamic scene viewing, we could not apply traditional fixation/saccade parsing that would distort the relationship between gaze and screen coordinates. Instead, the 1,000-Hz raw gaze recording was sampled down to 30-Hz records of raw *X*/*Y* coordinates and pupil dilation for each eye at the start of a frame. The SR Research saccade parsing algorithm was then used to identify blinks (pupil missing) and saccades in the original 1,000 Hz data using a 50°/s velocity threshold combined with an 8,000°/s^2 acceleration threshold. The acceleration threshold ensures that smooth pursuit movements, which exhibit much lower acceleration, are not misclassified as saccades. The frame-based samples were then marked according to whether the corresponding sample in the raw gaze trace was identified as a blink, saccade, or non-saccadic eye movements, i.e. fixations, smooth pursuit, and optokinetic nystagmus. For simplicity, this group of eye movements will be referred to as *foveations* in all subsequent discussion. These foveations retain the movement that was present within the raw gaze samples and provide a more accurate representation of the visual features projected onto the fovea that may influence gaze location. The parsing of eye movements was performed separately for left and right eyes although all subsequent analysis was only performed on frame-based samples in which both eyes were in a foveation. The total number of binocular foveations analyzed in this study was 3,297,084.

Computation of Visual Features

In order to identify the contribution of visual features to gaze position, several visual features were investigated: luminance, colors, edges, corners, orientation maps, flicker, motion, and their respective contrasts. Each frame of a movie was processed to identify the variation in a particular feature dimension across that frame. The range of feature values was then normalized between 0 and 1 where 0 is set to the minimum value and 1 the maximum [13]. Such normalization of feature values is supported by neurobiological evidence of the non-linear single-cell behavior in the primary visual cortex [70]. Further, a second smaller scale taken from the weighted average of a 4 × 4 neighborhood of pixels (i.e. bi-cubic sampling) was performed, as neurobiological evidence suggests this is done in the primary visual cortex and also because it is

carried out in most saliency models [71]. The final feature map was then averaged across both scales.

To calculate the selection of visual features for an individual foveation, 2° and 4° circular patches were computed around each foveation, and the means of these values were stored for each frame. For our results, we noticed minimal differences between 2° and 4° and thus only report the results employing 4-degree patches. We also investigated local contrast for each feature defined as the standard deviation of image pixels within these circular patches (denoted 'Std' in the results). This measure has been proposed for the luminance channel as a measure of the perceptual contrast in natural images [72, 73], linked to salience in eye movement studies [13, 14], and used for actual computational saliency models [48, 50]. Contrast has also been motivated as guiding bottom–up attention across all feature channels and is suggested to be more important than actual feature strength in guiding attention [19, 74, 75].

Static Features

Luminance and Color

The study of luminance, color, and their respective retinotopic gradients (contrast) as a predictor or major contributor of the human visual salience map is well documented [13, 21, 76] and typically employed in computational models of saliency [71, 77]. In our investigation of visual features, we separated luminance and color from a 3-channel red, green, blue (RGB) image encoding by making use of the 1976 CIE $L^*a^*b^*$ (CIELAB) color-space convention defined in the ICC profile specification.[1]

CIELAB allows the use of separating color perceptions into 3-dimensional space where the first dimension, L^*, specifies Luminance (Lum), and the other two dimensions, a^* and b^*, specify color opponents for Red-Green (RG) and Blue-Yellow (BY), respectively. When the color channels a* and b* are achromatic, (i.e. both 0), L^* extends values along the grayscale. We made use of the specification implemented in Matlab's Image Processing Toolbox with an example shown in Fig. 1.

Edges

Considering the neurobiological evidence of early-vision supporting lines, edge, contour, and center-surround operators [19, 26], the Sobel edge detector is an ideal binary operator for detecting edges in images. It has also been previously investigated as the primary feature employed in a simple measure of saliency [78] and as part of biologically inspired saliency maps [79, 80]. Sobel edge detection performs a 2-dimensional spatial gradient measurement on a luminance image using a pair of 3 × 3 pixel convolution masks and an approximation to the gradient defined by:

$$G_x = \begin{bmatrix} -1 & 0 & +1 \\ -2 & 0 & +2 \\ -1 & 0 & +1 \end{bmatrix}, \quad G_y = \begin{bmatrix} +1 & +2 & +1 \\ 0 & 0 & 0 \\ -1 & -2 & -1 \end{bmatrix}, \tag{1}$$

$$|G| = |G_x| + |G_y| \quad \text{(Sobel Edge Detection)}$$

where G_x is the horizontal operator, G_y is the vertical operator, and $|G|$ is the approximation used as the edge map [81]. A threshold parameter also controls which edges are selected in the output edge map, throwing away all edges above the threshold.

Corners

Complex features such as line-ends or corners where angles in lines or sharp contours occur have been shown to be part of early human visual processing [82] as well as shown to be more salient than regions with purely straight edge or simple feature stimuli [18]. Harris corners are well motivated as corner detectors in the computer vision community as they are invariant to rotation, scale, illumination, and image noise [83]. Noble [84] also explains how the Harris corner detector estimates image curvature and can characterize two-dimensional surface features such as junctions.

The Harris corner detector modifies the Moravec interest operator [85] by using a first order derivative approximation to the second derivative. The algorithm uses autocorrelation of image patches around an image pixel to find a matrix A, denoted as the Harris matrix:

$$A = \sum_u \sum_v w(u,v) \begin{bmatrix} I_x^2 & I_x I_y \\ I_x I_y & I_y^2 \end{bmatrix} \text{(Harris Corner Detection)} \tag{2}$$

where I_x and I_y are image gradients. Eigen values of this matrix correspond to a low-contrast pixel (both Eigen values are low), edge pixel (only one Eigen value is high), or corner pixel (both Eigen values are high) label for the given pixel depending upon their relationship [86]. We considered only the case depicting corners. An example can be seen in Fig. 2.

Orientation Maps

Neurons in the primary visual cortex have been shown to be selective to grating patterns tuned to different

[1] ICC.1: 2001-4, www.color.org.

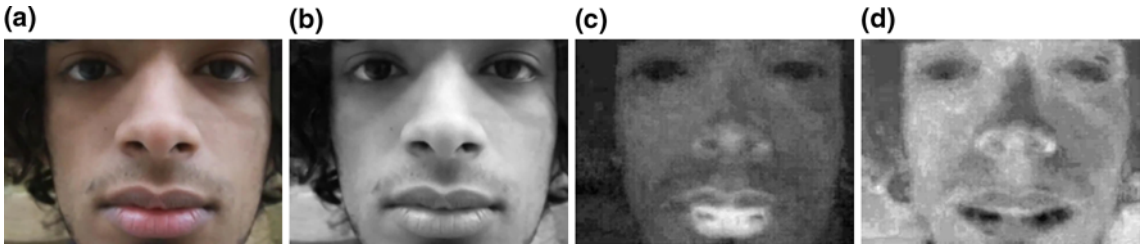

Fig. 1 **a** Original image of frame 1975 of video 24 ('Video Republic' http://www.demos.co.uk/publications/videorepublic); **b** L^* image depicting luminance (Lum); **c** a^* image depicting red/green opponent colors (RG); **d** b^* image depicting blue/yellow opponent colors (BY)

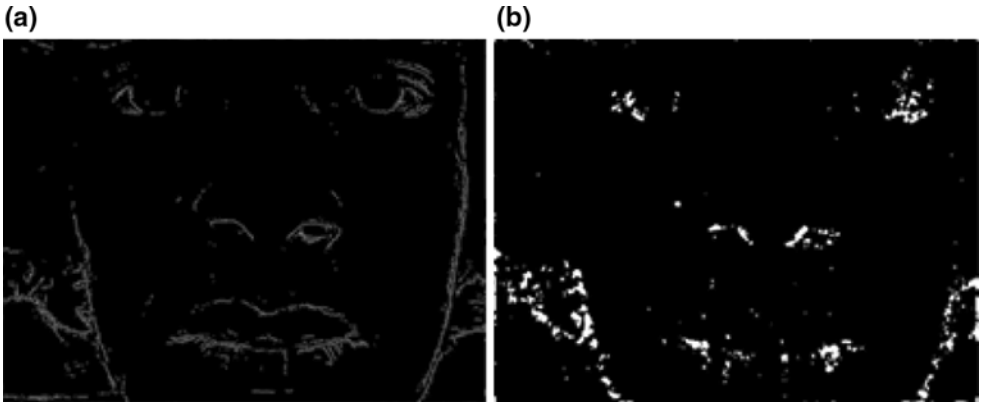

Fig. 2 **a** Edge map using Sobel edge detection; and **b** Harris corner detection map for the luminance image in Fig. 1b

orientations and scales [87, 88]. The uses of Gabor maps as replicating these orientation maps are highly motivated in scene perception, as they closely resemble the response properties of cortical cells [88, 89]. These maps are also often used in computing orientation maps over a number of scales in computational saliency models [50, 71].

To create a Gabor map, a luminance image is convolved with a "patch" defined by a log-Gabor function resulting in high values selective to certain orientations of edges. They are computed similarly to the Sobel operator through convolution though using a Gaussian kernel multiplied by a sinusoid instead of a gradient approximation. First, a radial map is computed like in Fig. 3a. This filter is the result of multiplying a Gaussian kernel with a sinusoid, and it controls the frequency band at which the kernel will respond to. The angular component of the filter shown in Fig. 3b controls the filter's orientation response. After multiplying the two together, the filter is created as in Fig. 3c. By taking the inverse Fourier transform of the filter, the even and odd symmetric components are taken from the real and imaginary components of the filter, respectively (shown in Fig. 3d and e).

These two filters are "summed" together in frequency domain allowing one to multiply the image in frequency domain in order to create an "orientation-map" image. The complex result of the convolution encodes both magnitude and phase portions of the response. For our purposes, we were only interested in the magnitude portions and simply took the absolute value of this result, ignoring the phase result. Further, we computed feature maps along four different orientations of log-Gabor patches: 0°, 45°, 90°, and 135°(examples in Fig. 4).

Dynamic Features

When viewing a film, a sequence of images gives the viewer a convincing impression of motion. These static frames are interpreted by the visual system to arrive at the perception of a continuously moving image. The phenomenon of apparent motion has been investigated in a number of studies that suggest the visual system performs feature matching [90–92] or temporal filtering [93]. We included two dynamic visual features shown to play a significant role in the visual system.

Flicker

Abrupt changes in luminance, or flicker, have been shown to pop out independently of observer intentions [94]. It has also been shown that two separate temporal channels for flicker exist as a low-pass and band-pass filter [95]. For our band-pass filter, we took the approach of previous research and simply computed the absolute difference between the current and previous frames and termed this 'Flicker' in

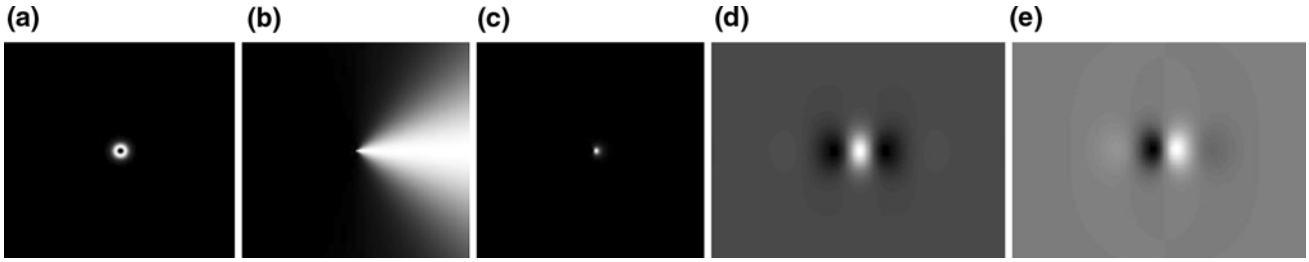

Fig. 3 The process for creating a log-Gabor kernel for 0° (*left* to *right*): **a** the radial map computed from multiplying a sinusoid with a Gaussian kernel; **b** the orientation of the kernel set for 0°; **c** the result of multiplying the radial (**a**) and orientation (**b**) maps; **d** the even symmetric component of the log-Gabor filter taken from the real part of the inverse fourier transform of the kernel; **e** the corresponding odd symmetric component taken from the imaginary component of the kernel

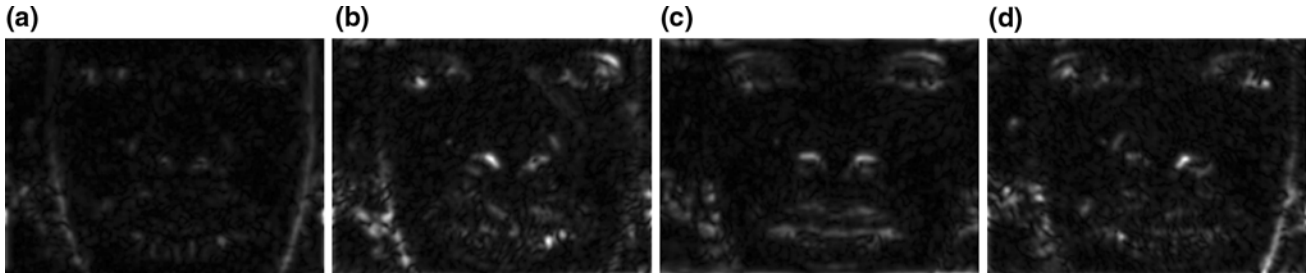

Fig. 4 Gabor-oriented maps for **a** 0°, **b** 45°, **c** 90°, and **d** 135° for the luminance image in Fig. 1b

our results section [19, 48]. As a low-pass filter, we used the maximum of the previous 5 absolute frame differences in order to capture slower frequency flickers (e.g. long-term change) and termed this 'Flicker-n'.

Object Motion

Cortical analysis of motion shows that the majority of V1 cells have selective response to motion in different orientations before sending their output to the medial temporal cortex [68]. It thus does not seem surprising to find that evidence based on search efficiency has shown that our visual system is able to notice moving objects even if we are not looking for them. Phenomena associated with parts of a scene that attract our attention are often given the label "pop out". Rosenholtz [75] has investigated these phenomena in the context of motion by creating a measure of saliency based on the extent to which the motion of a scene differed from the general pattern of the scene. She showed that a simple model measuring motion outliers can detect motion pop out phenomena reliably. As well, Itti and Baldi [77] have incorporated measures of motion into the most recent versions of the iLab Neuromorphic Vision C++ Toolkit for their saliency computations. We investigated this feature dimension by employing a classic computational vision algorithm for finding the motion of every pixel in a scene.

Horn and Schunck [96] optical flow is a differential method for calculating motion vectors in a brightness image. The flow of an image, I, is defined by:

$$f = \int \left(\left(\begin{bmatrix} I_x \\ I_y \end{bmatrix} \begin{bmatrix} V_x V_y \end{bmatrix} + I_t \right)^2 + \alpha \left(|\nabla V_x|^2 + |\nabla V_y|^2 \right) \right) \mathrm{d}x\mathrm{d}y \quad \text{(Optical Flow)} \tag{3}$$

where I_x, I_y, and It are the image derivatives, and V_x, and V_y are the components of optical flow in the x (U in vector notation) and y (V in vector notation) direction, respectively. This method is often referred to as a global method for calculating the optical flow, as the energy constraint (the first term in Eq. 3) assumes gray value constancy and does not depend on local image patches e.g. [97]. The energy equation includes a second term known as the "smoothing" term in order to smooth flow where distortions in the flow occur. This leads to better performance at filling in "gaps" left from moving objects with similarly textured regions than local methods.

In calculating our feature map, we discarded the vector component of flow in opposing directions and only considered their magnitudes as we were interested in response of motion and not their orientations. For example, −5 and +5 horizontal flow (denoted U-flow) corresponds to flow in the left and in the right direction, respectively. We disregarded this distinction and considered both as U-flow with

magnitude 5 (and similarly, with vertical or *V*-Flow). Examples are shown in Fig. 5.

Results

Visual Features at Baseline Foveations Versus Actual Foveations

To account for intrinsic variations in each film as well as central bias, we created a baseline measure by sampling with replacement from the distribution of all subject binocular foveations for each video similar to Henderson et al. [8] (see Fig. 6 for distributions). Thus, for each frame, baseline foveations were sampled with replacement from the distribution of all foveations across the duration of the movie. The number of baseline foveations sampled for each frame matched the number of valid actual foveations for that frame. Examples of actual subject and baseline foveations are shown in Fig. 7.

Selection of Visual Features During Dynamic Scene Viewing

In order to assess the selection of visual features, we followed the approach of previous research [15, 47, 52] by employing a signal detection framework based on the Receiver Operator Characteristic (ROC) curve [99]. This metric has a number of benefits when investigating fixated feature values: (1) capability of accounting for the variability of actual and baseline foveations, (2) independence from the number of data points used, (3) ability to recover the non-linear statistics of different visual features [98] via a dense sampling (i.e. more samples of signal/noise ratio), (4) accounts for the bias of photographers to place salient objects closer to the center of the composition [15], and (5) accounts for the distribution of foveations toward the center of an image by comparing actual foveations against a sampled baseline (see Fig. 6 for example foveation distributions, and Fig. 7 for example baseline foveations).

We employed the ROC in order to specify how well actual foveations (signal) could be separated from baseline foveations (noise) on each feature dimension. Each feature map was systematically thresholded from its minimum to maximum value. At each threshold, actual and baseline locations were identified as either having mean values above ("1") or below the threshold ("0"). The correct labeling of an actual location as "1" signified a "hit" whereas "0" was a "miss". If a threshold also labeled a baseline location as "1" it constituted a "false alarm". If the systematic thresholding produced as many hits as false alarms, then the feature dimension could not be said to distinguish between the signal (actual locations) and the noise (baseline locations) and, therefore, could not predict foveation.

As many of the feature spaces contained heavily skewed distributions and no assumptions were made concerning the feature space distributions, we used 200 non-linearly spaced thresholds in order to recover the tail ends of the feature distribution and model a tighter fit to the underlying ROC curve. Plotting a false alarm rate (baseline foveations as a "1") versus an actual hit rate (actual subject foveations as "1") provided a ROC curve describing the nature of the signal noise ratio across all thresholds. A feature dimension that performed at chance at separating signal from noise would thus create a straight line with hit rate being identical to the false alarm rate, i.e. a gradient of 1. By comparison, if a feature increased in its ability to discriminate actual from sampled foveation locations, the line would curve toward (0, 1). The greater the curve, the greater the area under the curve (AUC), and the greater the ability of a feature to discriminate between hits and false alarms. Thus, the curve can be accurately summarized by its AUC where 0.5 corresponds to chance (a linear line), and 1.0 corresponds to a perfect discrimination.

We classified attended visual features by investigating the AUC of a ROC analysis. Table 1 shows the results computed based on Fig. 8. A number of interesting findings were present. Luminance, Red/Green, and Blue/Yellow were just above chance although their respective standard deviations were much higher suggesting both luminance

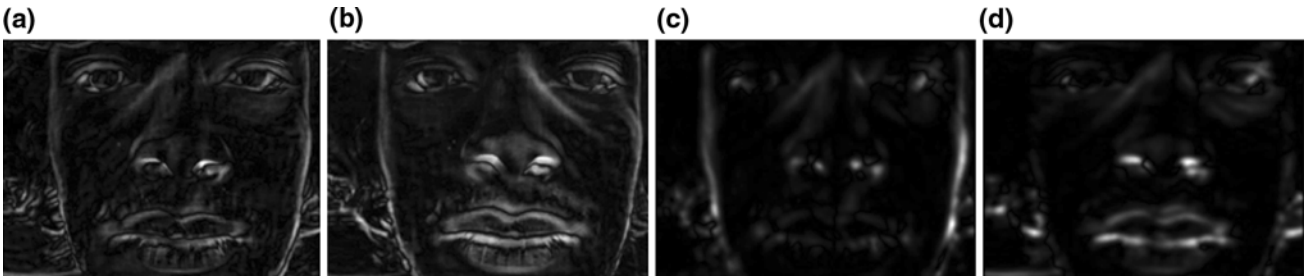

Fig. 5 **a** High-pass flicker (Flicker); **b** low-pass flicker (Flicker-N); **c** horizontal optical flow (*U*-Flow); **d** vertical optical flow (*V*-Flow) for the frame in Fig. 1a

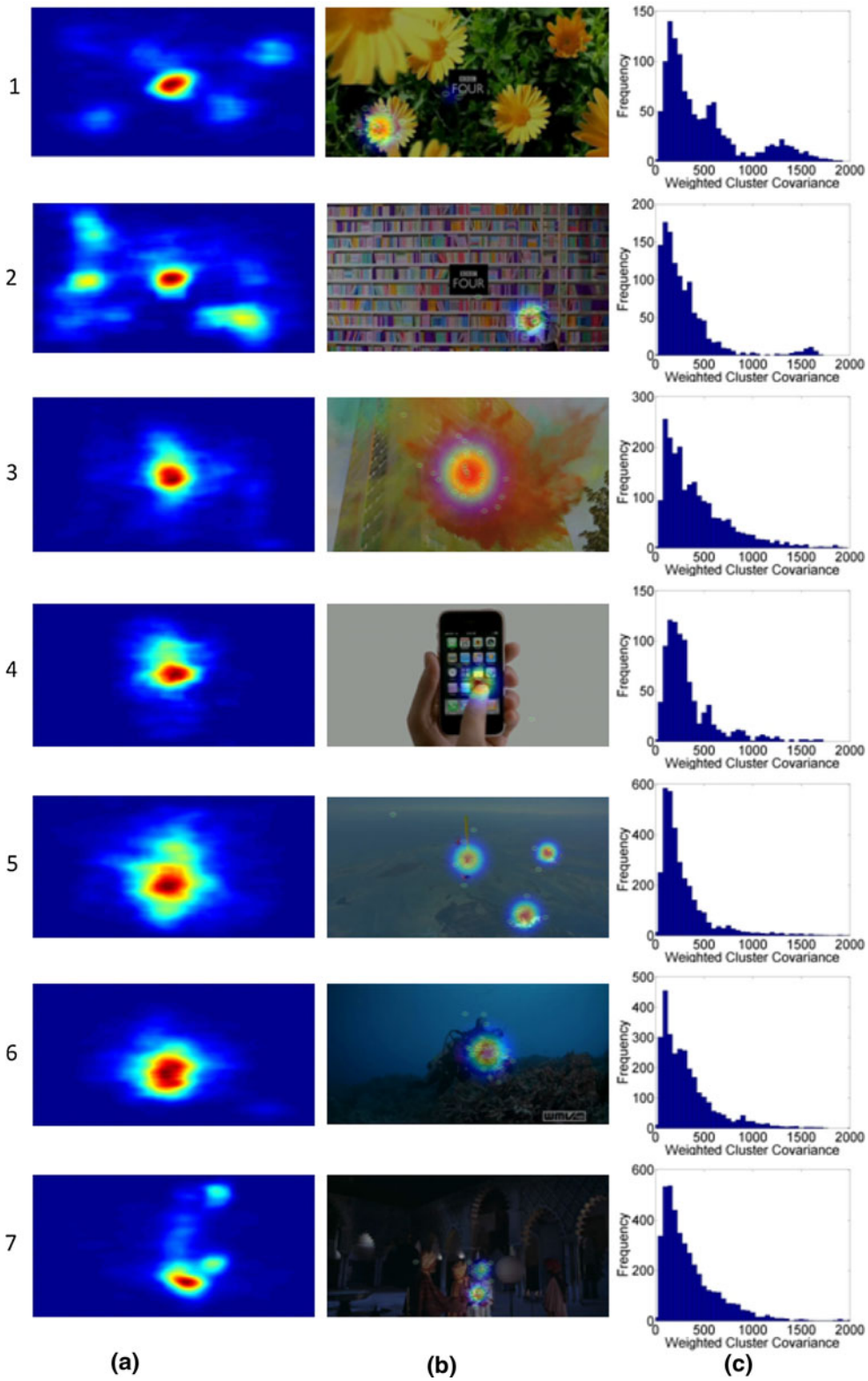

Fig. 6 **a** Binocular foveation distributions for each movie represented as heat maps (normalized 0–1, blue-red). **b** Example scenes for each movie with clustering of gaze and individual gaze locations overlaid; **c** histograms of weighted cluster covariances for each film. (see Appendix 2 for the remaining films used)

and opponent color contrast as important selected features. Edges performed at chance though this was likely because of the very sparse response of the edge-maps at the selected kernel size of 3 × 3 and selectivity threshold of the Sobel implementation.

We found little differences between orientations and their standard deviations though both feature sets were selected more than Luminance, Red/Green, and Blue/Yellow. High-pass Flicker performed just below the Gabors though the low-pass measure of Flicker, Flicker-N,

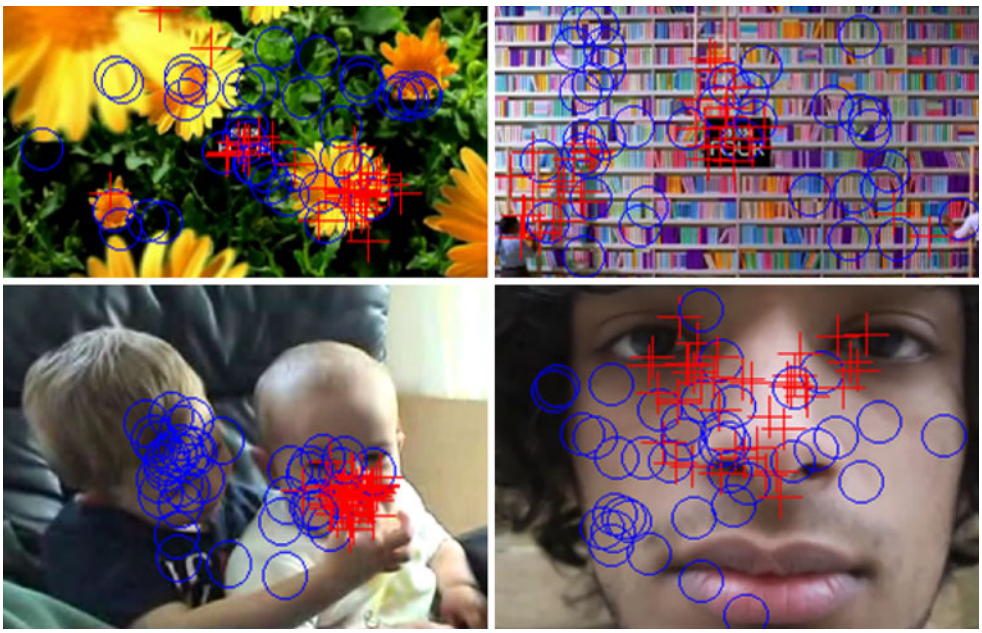

Fig. 7 Example actual (*cross*) and baseline (*circle*) subject foveations for videos 1, 2, 15, and 24 (*clockwise from top left*)

Table 1 The area under the receiver operator characteristic curve (AUC) for feature values 4° around gaze locations

Feature	AUC
Luminance	0.526377
Luminance Std Dev	0.630167
Red/Green	0.546701
Red/Green Std Dev	0.606843
Blue/Yellow	0.531026
Blue/Yellow Std Dev	0.608749
Sobel edges	0.530066
Sobel edges Std Dev	0.530062
Gabor at 0°	0.604528
Gabor at 0° Std Dev	0.608238
Gabor at 45°	0.608014
Gabor at 45° Std Dev	0.61033
Gabor at 90°	0.596378
Gabor at 90° Std Dev	0.599987
Gabor at 135°	0.607202
Gabor at 135° Std Dev	0.609411
Harris corners	0.636152
Harris corners Std Dev	0.646601
Flicker	0.584435
Flicker Std Dev	0.589377
Flicker (N-prev)	0.619877
Flicker (N-prev) Std Dev	0.645487
U optical flow	0.670323
U optical flow Std Dev	0.675288
V optical flow	0.66854
V optical flow Std Dev	0.673837

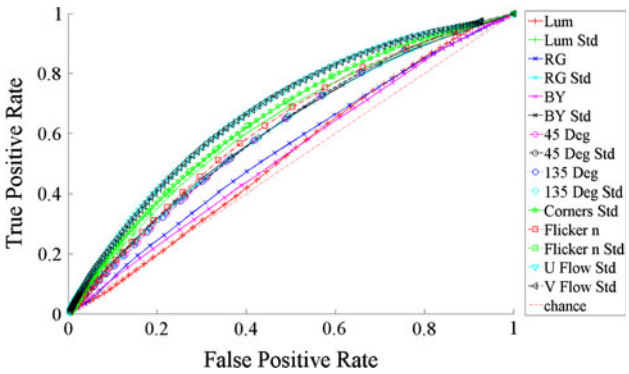

Fig. 8 ROC curves for a selection of the features @ 4°. Higher curves toward point (0, 1) are better. Chance is 0.5. Best viewed in the online version of the publication in color. Refer to Table 1 for all feature results

as well as its standard deviations performed on par with Luminance Std Dev, Red/Green Std Dev, Blue/Yellow Std Dev, Harris Corners and Harris Corners Std Dev, suggesting a higher selection toward motions occurring over a longer interval. Optical flow features (U/V flow and their standard deviations) performed the highest (0.67, 0.68, 0.67, 0.67) of our investigated features. This is strong evidence for motion as the most predictive visual feature of foveations during dynamic scene viewing.

Within Subject Categorical Analysis Between Tight and Loosely Clustered Gaze

The phenomena of attention capture have been studied in the context of natural scene viewing suggesting that abrupt

onsets of distinct objects, unique colors or shapes, or certain patterns of motions are particularly selective of attention [43]. During these involuntary moments of attention capture, viewers are thus expected to cluster in similar locations of a natural scene. We investigated a measure of clustering of eye movements in order to infer whether feature values are more predictive of subject eye movements during moments of tight clustering.

Only a few known studies have looked into clustering eye movements. Privitera and Stark [100] compared actual and simulated foveations using *k*-means clustering. Latimer [101] used a form of *k*-means based on histograms of foveation durations in an effort to classify partitions more robustly, although he comments that k-means clustering often produces inconsistent results. Santella and DeCarlo [102] quantified visual interest via a mean-shift clustering framework. Though this method is robust to noise and does not require the number of clusters a priori, it does require additional tuning of parameters based on temporal and spatial scales.

Reported success of density estimation via expectation/maximization [103] of a parametric family distribution in Sawahata et al. [59] prompted us to use mixture models as our clustering method. Sawahata et al. investigated an entropy measure calculated from the log likelihood of a mixture model in order to determine viewer comprehension during dynamic scene viewing. This method when combined with model selection and enough data points can produce consistent results that are robust to noise and does not require the number of clusters a priori (which is the main drawback of *k*-means clustering). A prior model of the distribution of data is required in order to accurately tune the parameters during expectation/maximization. We used Gaussians as our parametric prior since they have been shown to account for much of the variance in the center bias apparent in viewing strategy and photographer bias during dynamic image viewing [66]. The resulting model is more commonly known as a Gaussian Mixture Model (GMM).

GMMs represent a collection of unlabeled data points as a mixture of Gaussians each with a separate mean, covariance, and weight parameter. For our purposes, we used this model to classify moments of tight and loose clusters of eye movements across subjects by calculating the sum of the weighted cluster covariances (i.e. the sum over all cluster covariances weighted by the cluster weight). Note that by using model selection, the problem of over-fitting a model to noise, i.e. zero covariance Gaussians centered at fixations, is dealt with in the BIC term which penalizes the number of clusters. We refer the reader to Bishop [103] and Sawahata et al. [59] for more details on GMM modeling and model selection. A few example stills are shown in Fig. 9 depicting the GMMs extracted from this algorithm.

Fig. 9 Example stills from clustering binocular eye tracking data on video 16. Blue values correspond to 0.0 and red to 1.0. The first example still uses the values of the GMM as an alpha-map layer providing a 'peek-through' effect. Notice the robustness to noise given the large number of data samples in the first still (original movie image of Ice Age 3 Trailer Copyright Twentieth Century Fox)

We investigated the correlation between frames eliciting tightly clustered data with the low-level features that encode them. We first classified all frames by their weighted cluster covariance. Then, we categorized "tightly clustered" (low covariance) and "loosely clustered" (high covariance) frames in order to see whether actual subject eye movements were more or less predictive of low-level features. If visual features are correlated with where we attend, then moments when everybody looks in the same place should also correlate with a peak in the feature space. As well, we should expect to find less influence of visual features during moments when there is less synchrony between viewers (i.e. high covariance). To test this hypothesis, we used Gaussian Mixture Models (GMMs)

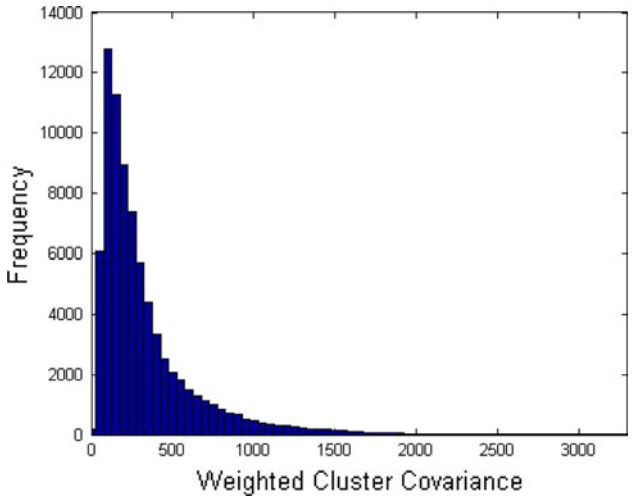

Fig. 10 A plot depicting a histogram distribution of all frames weighted covariance measure. To classify tight and loosely clustered frames, we used the median of the distribution of all frames for all movies weighted covariance value, which is centered at 230 (mean 360, sigma 330)

using a Bayesian Information Criterion (BIC) model selection on the frame-by-frame eye movements across all subjects.

To define a moment of synchrony, we investigated the distribution of the weighted Gaussian covariance. This measure has the benefit of measuring the distribution of eye movements in a given frame (in terms of the covariance) as well as indicating the strength of each cluster to model eye movements (in terms of the weight parameter). The histogram of the weighted covariances for each film (depicted in Fig. 6 and Appendix 2) clearly indicates a large degree of variation in the degree of clustering. Some films, such as film 15 exhibit tight clustering throughout their entire viewing time, whereas other films, such as film 26 exhibit very little clustering.

To classify tightly and loosely clustered frames, we used the median of the distribution of all frames for all movies' weighted covariance value, which is centered at 230 (mean 360, sigma 330; see Fig. 10). Taking only the frames greater than and less than the median, we were able to consider whether any features could be distinguished when compared to a random baseline measure in a categorical analysis of tightly and loosely clustered frames.

Splitting gaze according to the degree of clustering revealed a systematic increase in the ability of all visual features to discriminate actual from baseline foveations for tight clusters. AUC values were higher for tight clusters than loose clusters in all features. For example, vertical optical flow AUC values increased from 0.63 in loose clusters to 0.71 in tight ones, indicating that during these moments 71% of actual gaze locations could be discriminated from baseline locations by this feature alone. This suggests that the selection of visual features is more predominant as eye movements across multiple subjects are clustered tightly together than during loosely clustered scenes. As in the comparison with baseline subjects across all frames, we found the most significant AUC values for motion. As well, the standard deviation of each feature had a higher response than the feature strength alone (Table 2).

Table 2 The area under the curve (AUC) for each feature dimension split according to weighted cluster covariance

Feature	Loose clusters (AUC)	Tight clusters (AUC)
Luminance	0.505682	0.545678
Luminance Std Dev	0.597268	0.66307
Red/Green	0.515643	0.576606
Red/Green Std Dev	0.578396	0.633503
Blue/Yellow	0.519821	0.542573
Blue/Yellow Std Dev	0.582418	0.634017
Sobel edges	0.520351	0.53968
Sobel edges Std Dev	0.520349	0.539674
Gabor at 0°	0.57853	0.630239
Gabor at 0° Std Dev	0.581526	0.634526
Gabor at 45°	0.579087	0.636106
Gabor at 45° Std Dev	0.580594	0.639148
Gabor at 90°	0.568905	0.622719
Gabor at 90° Std Dev	0.571076	0.627879
Gabor at 135°	0.578521	0.635135
Gabor at 135° Std Dev	0.580133	0.638033
Harris corners	0.602542	0.669791
Harris corners Std Dev	0.612087	0.680933
Flicker	0.560667	0.60797
Flicker Std Dev	0.564554	0.614068
Flicker (N-prev)	0.589983	0.650598
Flicker (N-prev) Std Dev	0.61298	0.678218
U optical flow	0.636065	0.705184
U optical flow Std Dev	0.640588	0.710575
V optical flow	0.630426	0.706752
V optical flow Std Dev	0.635424	0.712136

Loose clusters and tight clusters are defined as $>$ are $<$ the median weighted cluster covariance (230), respectively

Selection of Visual Features as a Function of Clustering

The median split of cluster covariance indicated that tighter clusters correspond with higher AUC values. To examine this relationship further, the distribution of cluster covariances was further subdivided into seven bins of width 75 and a maximum of 525 (careful examination of the range of weighted cluster covariances across movies indicated very few moments above 525; Appendix 2).

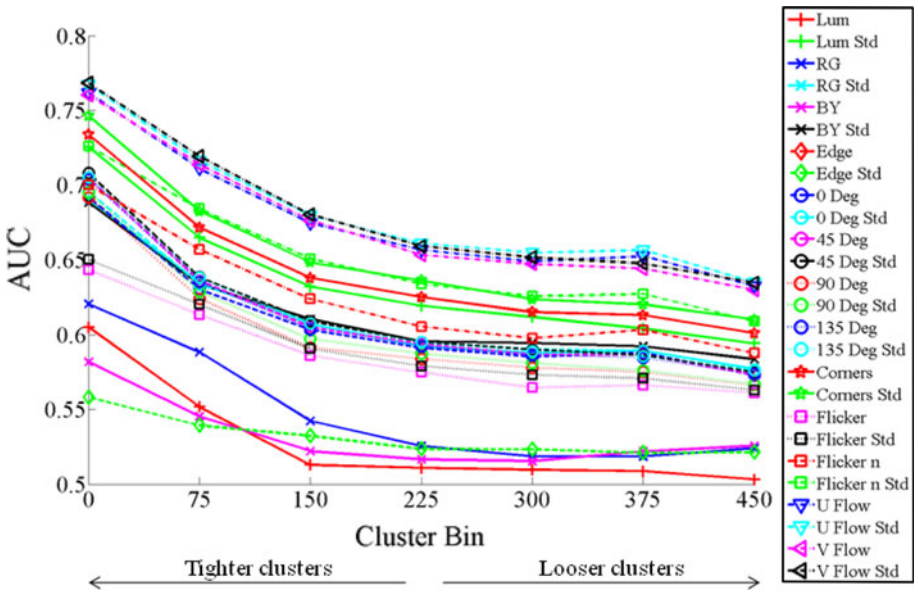

Fig. 11 Area under ROC curves (AUC) as a function of weighted cluster covariance (bins = 75)

The AUC results are presented graphically as a function of each bin in Fig. 11. The figure clearly demonstrates an inverse curvilinear relationship between weighted cluster covariance and AUC. Each feature presents a clear trend toward higher AUC values for smaller bin sizes, suggesting that as clusters are tighter, the selection of visual features are more predominant. Notably, the order of the most predominantly selected visual features stays similar in each bin size with motion topping the list in each bin. For example, during moments of tightest clustering (0–75), the percentage of actual locations correctly discriminated from baseline locations by vertical flow increases from ~64 to 77%.

The influence of Cinematic Cuts on the Selection of Visual Features

Previous research has suggested that a strong central bias exists based on photographer bias and viewing strategy [65, 66] producing high inter-observer consistency, i.e. a metric determining the "spread" in eye movements, immediately following a cinematic cut. Further, Carmi and Itti's [48] research suggests that the selection of saliency and motion contrasts is highest during high inter-observer consistency following semantically unrelated MTV-style jump cuts. However, our content did not control for top–down behavior and thus would include influences from prior scene knowledge and continuity editing. That is, scene content may or may not be related on either side of a cinematic cut.

Given previous research findings, a possible explanation for the higher selection of visual features during tightly clustered scenes is that these clusters may be most predominant following a cinematic cut where during semantically unrelated content, visual feature selection has been shown to be the highest. As such, our results in the previous section could either have been indicative of (1) photographer bias and viewing strategy, where tightly clustered eye movements following cinematic cuts explain higher selection of visual features during dynamic scene viewing; (2) spontaneous clustering of eye movements during ongoing dynamic scene viewing; or (3) both 1 and 2.

In order to investigate this issue further, we took the same approach as Carmi and Itti [48] in investigating the first saccades following an abrupt cinematic cut. We hand-coded every cinematic cut for each of our 26 movies excluding those with cuts that are not distinguished by abrupt changes to a single composition (e.g. multiple composite videos or alpha/chromaticity blending). Plotting the weighted cluster covariance as a function of time following a cinematic cut revealed a tendency for viewers to cluster tightly together with a mean weighted covariance value approaching 250 during the first 533 ms (Fig. 12). Further, plotting the Euclidean distance of foveations to the center of the display revealed a central bias 333 ms following a cut (Fig. 13).

To investigate whether the peak in feature selection was caused by the tight clustering immediately following a cut, we analyzed three time periods such that the center of these bins were closely centered to the observed clustering and central bias at 333 and 533 ms: 0–200 ms, 200–400 ms, and 400–600 ms following a cut. The results show that, contrary to the hypothesis that clustering following cuts is the primary explanation for higher selection of visual features during dynamic scene viewing, there is no noticeable peak close to the previous AUC value in feature selection for any degree of clustering immediately following the cut (0–200 ms) or in either of the other two time windows

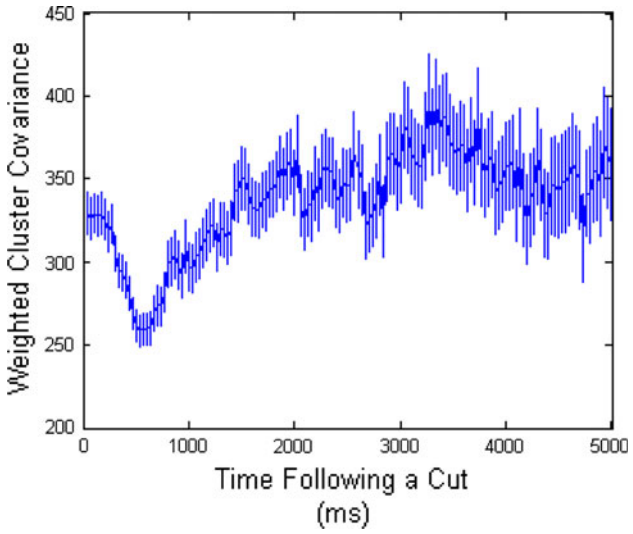

Fig. 12 Weighted cluster covariance as a function of time since a cut. Error bars represent ±1 SE

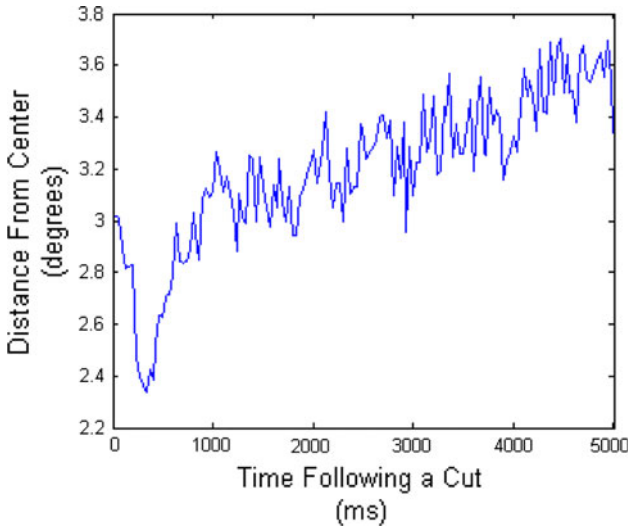

Fig. 13 Euclidean distance between foveations and screen center as a function of time since a cut

(Fig. 14). The ranking of selection for feature dimensions remains the same, with motion features contributing most to gaze location, but the effect of greater feature selection during tighter clustering behavior is greatly weakened if not entirely gone. This suggests that the tight clustering observed immediately following cuts in our film corpus is caused by a central tendency (Fig. 13) and not exogenous control by visual features. Given the absence of a strong relationship between clustering and feature selection immediately following cuts, the relationship observed throughout films (Fig. 11) cannot be fully attributed to cuts and appears to mostly occur spontaneously during ongoing dynamic scenes.

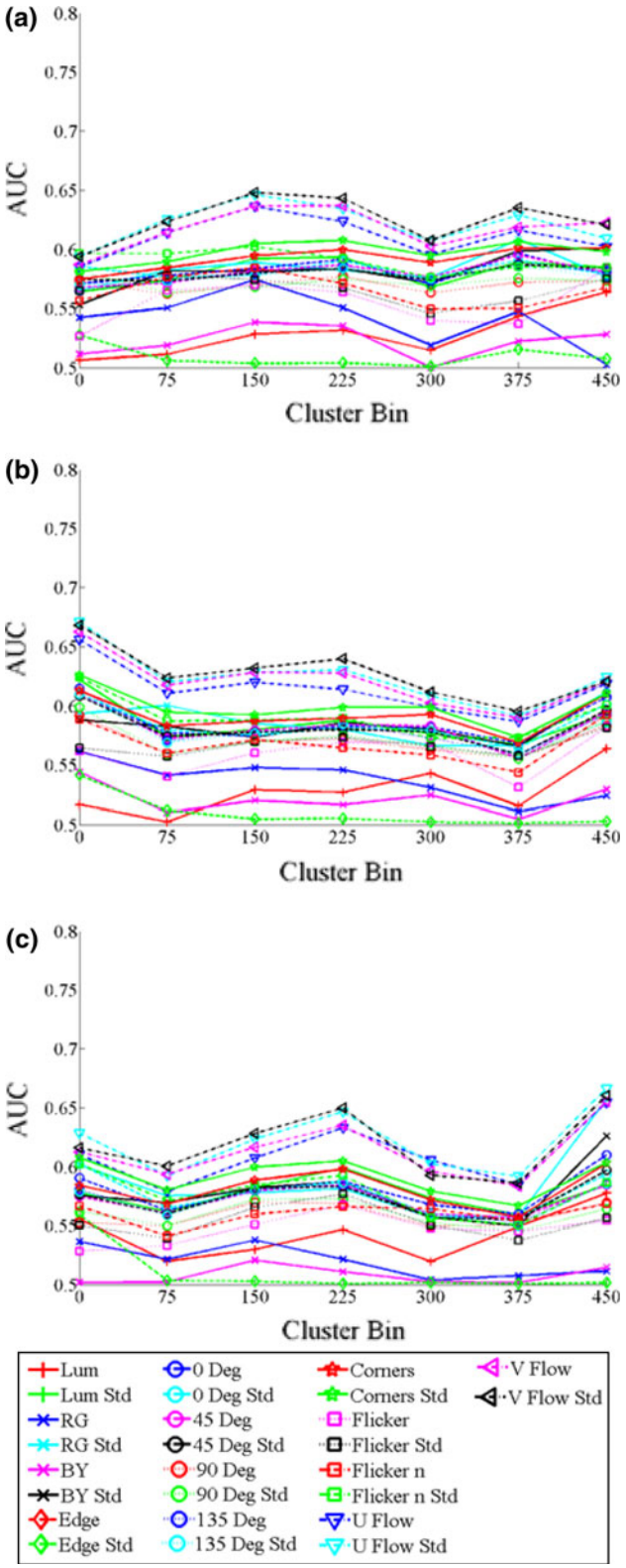

Fig. 14 AUC presented as a function of weighted cluster covariance at time points **a** 0–200 ms, **b** 200–400 ms, and **c** 400–600 ms following a cut

Discussion

The present study investigated the contribution of visual features to gaze location during free-viewing of dynamic scenes using a signal detection framework. The results indicated that foveated locations could be discriminated from control locations by mid-level visual features with motion contrasts as the strongest predictors, confirming previous evidence that motion is the strongest independent predictor of gaze location in dynamic scenes [48, 50]. The next strongest predictors following motion were corners suggesting a strong role in mid-level visual features to predict gaze location. High-pass flicker performed just below Gabor orientations although the low-pass measure of flicker, flicker-n, as well as their standard deviations performed on par with the standard deviations of luminance, color, and corners, suggesting a stronger selection for changes occurring over a longer interval than shorter ones. Low-level visual features such as luminance and color were not able to discriminate foveated from non-foveated locations as their AUC value was around chance, 0.5. However, as their respective contrasts (i.e. standard deviations) were much higher, this would suggest that both luminance and opponent color contrast are important selected features.

Edges performed at chance although a number of issues were present. First, the kernel size of 3×3 may not have been ideal to produce a range of edge values. Second, the process of thresholding edge values from the Sobel operator may also not have been ideal and instead a non-maximum suppression and hysteresis procedure would produce edges closer to perceptual boundaries. Torre and Poggio [104] also note that filtering of a sampled image prior to differentiation is necessary to regularize the problem of computing derivatives in an intensity image. This could be achieved by a band-pass (e.g. sinc or prolate) or minimal uncertainty (e.g. Gabor or Hermite function) filter. However, each filter is noted to have different merits and trade-offs. Further, a number of other edge operators are predominant in the computer vision community based on gradients, phase congruency, or second derivatives, again each with their own merits and trade-offs. These issues could be investigated in more depth in future studies to reproduce the selection of edges by gaze as shown in previous static studies [7, 8, 15, 105, 106].

Gaze Clustering

The selection of all visual features increased as the degree of clustering of gaze increased. During these moments, the ordering of feature selectivity remained the same, but their degree of contribution increased considerably. For example, motion increased from an overall average AUC of $\sim$0.64 to 0.77 during moments of tightest clustering. This indicates that during these moments 77% of foveated locations could be distinguished from control locations via motion information alone. On the face of it, this relationship between clustering and feature contributions to gaze would seem to suggest bottom–up gaze control: universal involuntary capture of gaze by a point of high motion. Such a causal interpretation was proposed by Carmi and Itti [48] for moments during dynamic scene viewing when all top–down influence was removed, e.g. immediately following a cut to a semantically unrelated dynamic scene. However, identifying similar moments in our stimuli revealed no relationship between visual features and gaze clustering during the first second following a cut. Instead, clustering following cuts seems to be caused by a tendency to saccade to the screen center. A similar central bias has previously been reported during dynamic scene viewing [52] and is thought to be due to compositional bias, e.g. framing focal objects at screen center, and a viewing strategy of using the screen center to reorient to new scenes [66]. Carmi and Itti [48] did not control for central bias in their analysis as their control locations were sampled uniformly across the screen. Subsequent analysis of similar videos in their lab showed that there was a strong central tendency immediately following a cut and they suggested that future studies should sample control locations from this centrally biased baseline in order to identify the independent contributions of visual features [66]. The ROC analysis performed in the present study uses such a centrally-based baseline by sampling from each participants own gaze locations at another time point in time during the same video. With the contribution of screen center subtracted from the analysis, we found no contribution of visual features to gaze clustering immediately following cuts.

Bottom–Up Versus Top–Down Control During Ongoing Dynamic Scenes

The moments of clustering observed in our study occurred spontaneously during ongoing dynamic scenes. We have previously observed this phenomenon and referred to it as *Attentional Synchrony* [60]. The increase in visual feature contributions during Attentional Synchrony may suggest that gaze is involuntarily captured by sudden unexpected visual features such as object appearances or motion onsets [43–46]. Bottom–up control of gaze by unexpected events in the real-world such as the sudden approach of a predator, car, or projectile has clear evolutionary advantages. However, it is difficult to separate the bottom–up influence of such visual events from top–down prioritization due to their *Cognitive Relevance* [8, 34, 107]. As visual features such as luminance, contrast, and edge density in scenes have been shown to correlate with the rated semantic informativeness of a location [8], gaze may be guided toward an object due to its cognitive relevance, and the corresponding peak in

feature values around foveation may simply be a by-product of this correlation. For example, a recent study by Vincent et al. [108] used mixture modeling to isolate the independent contributions of low and high-level visual features to fixations in static scenes. The authors found that low-level features in isolation contributed very little to fixation location compared to the much larger contribution of central bias and preference for foreground objects.

A quick survey of the visualized clusters observed in our study suggests that clusters often coincide with semantically rich objects such as eyes, faces, hands, vehicles, and text (see Figs 6, 7, 10 and Appendix 1 for examples). Gaze also appears to be allocated over time in response to visual events such as human bodily movements, gestures, conversations, and interactions with other humans and objects. Further, perception of complex visual events is known to operate in a predictive manner based on previous exposure to similar events [109] but is also predicted by discontinuities of motion [110, 111].

When visual events are recorded for presentation in Television or Film, scenes may be composed to focus attention toward the event by manipulating visual features such as lighting, color, focal depth, central framing, and motion of the object relative to the background and frame [112]. Such composed dynamic scenes were used in this and previous studies [48, 49, 51, 52, 66]. As such, the compositional manipulations of the image may increase the correlation between gaze and visual features though would not necessarily imply causation. A particular location may be foveated because it is cognitively relevant to the viewer and not because of a high contrast in visual features. The cognitive relevance of an object may remain even in the absence of distinct visual features. Static [113, 114] and dynamic scene studies [115] in which semantically rich regions have been filtered to remove visual features have shown that participants continue to attend to the semantically rich regions even though these regions are heavily obscured, further suggesting that top–down factors such as object semantics are the main contributors to gaze allocation.

Predicting Gaze Location in Dynamic Scenes

Is it possible to predict gaze location in dynamic scenes? An ideal model of gaze location in dynamic scenes would robustly locate the causal root of gaze allocation in terms of cognitively relevant scene semantics. This would entail robustly computing object and scene semantics relevant to a viewer's task and expertise given prior memory and encoding of the scene. However, the natural correlation between scene semantics and motion in natural scenes may provide a reasonably reliable method for predicting gaze location. In a natural dynamic scene viewed from a static vantage point (e.g. camera position), the only focused motion in the scene will be produced by animate objects such as people, animals, and vehicles. Identification of the motion created by these objects may provide a simple method of automatically parsing the objects from the background and identifying candidate gaze locations. The predictions of such a model will remain valid as long as (a) objects in the scene continue moving; (b) the background and camera remain stationary; and (c) top–down and bottom–up factors remain correlated such as during free-viewing. It is currently not known what effect the de-correlation of top–down and bottom–up factors would have on gaze allocation. If participants were instructed to search for an inanimate object, would this top–down instruction be able to completely override the bottom–up contribution of features such as motion? Only by pitting top–down and bottom–up factors against each other during dynamic scene viewing would we be able to understand their relative contributions and evaluate how reliable a model based solely on bottom–up features would be in predicting gaze location.

Acknowledgments The authors would like to thank members of the Edinburgh Visual Cognition laboratory including Antje Nuthmann and George Malcolm for their comments and feedback, and Josie Landback for running experiments. This project was funded by the Leverhulme Trust (Ref F/00-158/BZ) and the ESRC (RES-062-23-1092) awarded to John M. Henderson.

Appendix 1

See Table 3.

Table 3 List of videos used in this study

Number	Video type	Width	Height	Duration (s)	Cuts	ASL (s)
1	Advertisement	1,024	768	41	0	41
2	Advertisement	1,024	768	40	0	40
3	Advertisement	1,280	720	72	43	1.6
4	Advertisement	848	480	30	7	4.2
5	Documentary	1,280	720	109	13	8.4
6	Documentary	1,280	720	98	58	1.7
7	Documentary	1,280	720	152	11	13.1
8	Documentary	1,280	720	106	27	7.8
9	Documentary	1,280	720	86	14	6.1
10	Documentary	1,280	704	169	23	7.3
11	Game trailer	1,280	720	124	N/A	N/A
12	Game trailer	1,280	720	103	62	1.6
13	Game trailer	1,280	720	110	76	1.4
14	Game trailer	1,280	548	203	30	6
15	Home movie	960	720	55	0	55
16	Movie trailer	1,280	690	109	18	6
17	Movie trailer	1,280	688	99	94	1

Table 3 continued

Number	Video type	Width	Height	Duration (s)	Cuts	ASL (s)
18	Music video	704	576	27	N/A	N/A
19	Music video	1,024	576	216	N/A	N/A
20	Music video	1,280	720	43	N/A	N/A
21	News	768	576	102	23	4.4
22	News	768	576	66	16	4.1
23	News	1,080	600	85	N/A	N/A
24	News	960	720	209	N/A	N/A
25	News	768	576	217	31	5.3
26	Time-lapse	1,280	720	47	N/A	N/A

Columns left to right: Video number; Video Type; Width (pixels); Height (pixels); Duration (s); Number of cuts (n.b. N/A unable to calculate due to use of digital effects); Average Shot Length (ASL; s). Our study used 26 different films ranging a total of 549 edits used in the analysis of cinematic features, at 30 fps and 333 ms bins over 1 s (i.e. 5,490 frames of data per bin)

Appendix 2

Continuation of Fig. 6.

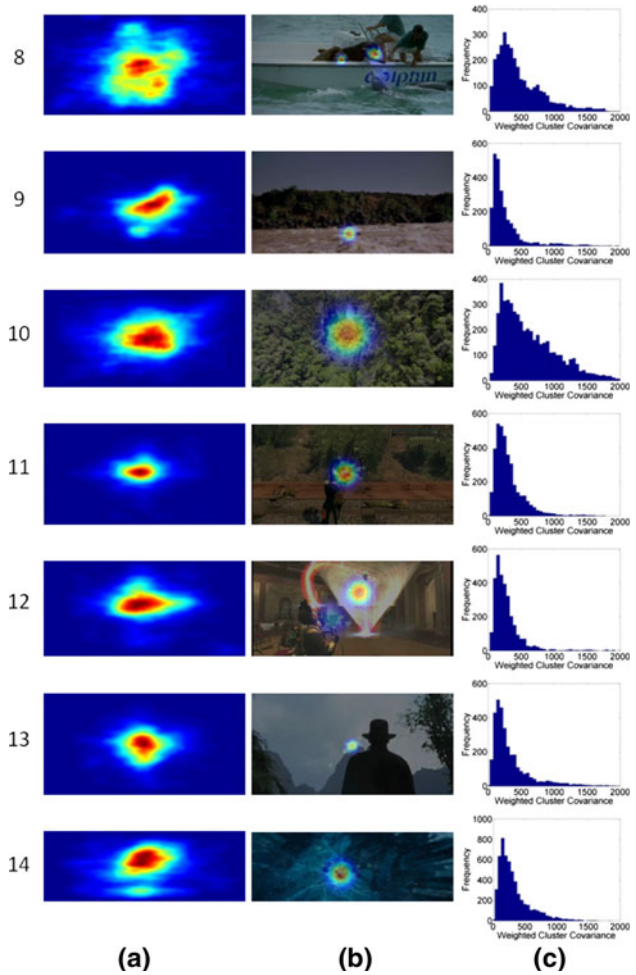

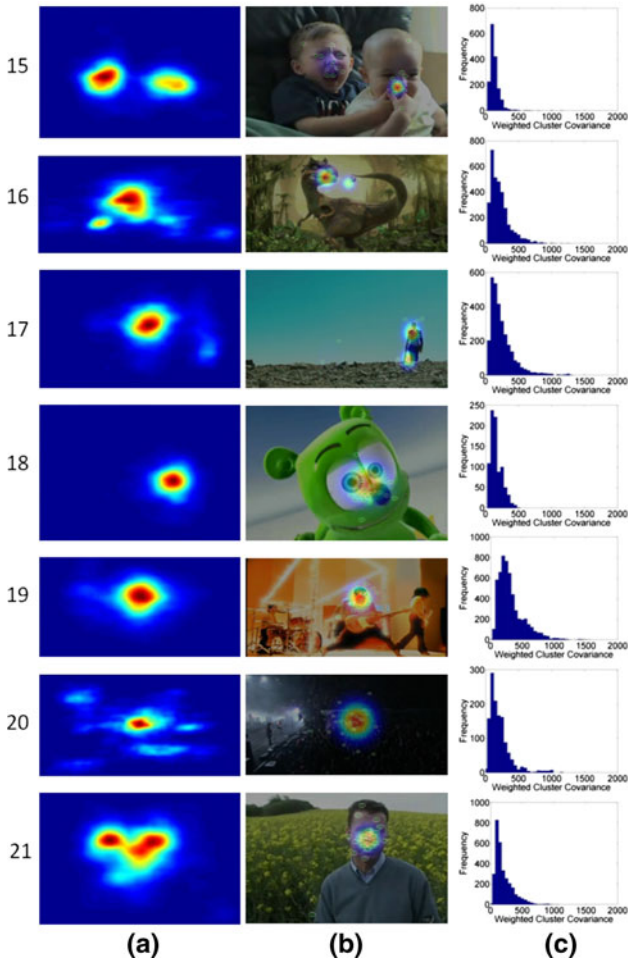

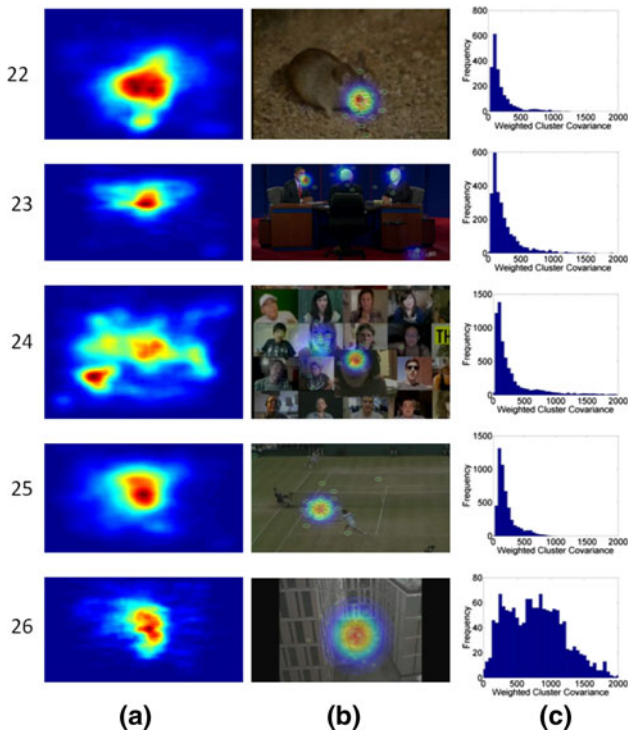

References

1. Findlay JM. Eye scanning and visual search. In: Henderson JM, Ferreira F, editors. The interface of language, vision, and action: eye movements and the visual world. New York, NY, US: Psychology Press; 2004. p. 134–59.
2. Findlay JM, Gilchrist ID. Active vision: the psychology of looking and seeing. Oxford: University Press; 2003.
3. Henderson JM. Regarding scenes. Curr Dir Psychol Sci. 2007;16(4):219–22.
4. Wolfe JM, Horowitz TS. What attributes guide the deployment of visual attention and how do they do it? Nat Rev Neurosci. 2004;5:1–7.
5. Buswell GT. How people look at pictures: a study of the psychology of perception in art. Chicago: University of Chicago Press; 1935.
6. Yarbus AL. Eye movements and vision. New York: Plenum Press; 1367.
7. Baddeley RJ, Tatler BW. High frequency edges (but not contrast) predict where we fixate: a Bayesian system identification analysis. Vision Res. 2006;46:2824–33.
8. Henderson JM, et al. Visual saliency does not account for eye movements during visual search in real-world scenes. In: van Gompel RPG, et al., editors. Eye movements: a window on mind and brain. Oxford: Elsevier; 2007. p. 537–62.
9. Krieger G, et al. Object and scene analysis by saccadic eye-movements: an investigation with higher-order statistics. Spat Vis. 2000;13(2–3):201–14.
10. Mannan S, Ruddock KH, Wooding DS. Automatic control of saccadic eye movements made in visual inspection of briefly presented 2-D images. Spat Vis. 1995;9(3):363–86.
11. Mannan SK, Ruddock KH, Wooding DS. The relationship between the locations of spatial features and those of fixations made during visual examination of briefly presented images. Spat Vis. 1996;10(3):165–88.
12. Mannan SK, Ruddock KH, Wooding DS. Fixation sequences made during visual examination of briefly presented 2D images. Spat Vis. 1997;11(2):157–78.
13. Parkhurst DJ, Niebur E. Scene content selected by active vision. Spat Vis. 2003;6:125–54.
14. Reinagel P, Zador AM. Natural scene statistics at the centre of gaze. Netw Comput Neural Syst. 1999;10:1–10.
15. Tatler BW, Baddeley RJ, Gilchrist ID. Visual correlates of fixation selection: effects of scale and time. Vision Res. 2005;45(5):643–59.
16. Parkhurst DJ, Niebur E. Texture contrast attracts overt visual attention in natural scenes. Eur J Neurosci. 2004;19:783–9.
17. Barth E, Zetsche C, Rentschler I. Intrinsic two-dimensional features as textons. J Opt Soc Am A Opt Image Sci Vis. 1998; 15:1723–32.
18. Zetzsche C, et al. Investigation of a sensorimotor system for saccadic scene analysis: an integrated approach. In: Feifer RP, editor. From animals to animats 5. Cambridge, MA: MIT Press; 1998. p. 120–6.
19. Itti L, Koch C. Computational modelling of visual attention. Nat Rev Neurosci. 2001;2(3):194–203.
20. Navalpakkam V, Itti L. Modeling the influence of task on attention. Vision Res. 2005;45(2):205–31.
21. Parkhurst D, Law K, Niebur E. Modeling the role of salience in the allocation of overt visual attention. Vision Res. 2002;42(1):107–23.
22. Pomplun M, Reingold EM, Shen J. Area activation: a computational model of saccadic selectivity in visual search. Cogn Sci. 2003;27:299–312.
23. Rao RPN, et al. Eye movements in iconic visual search. Vision Res. 2002;42(11):1447–63.
24. Sun Y, et al. A computer vision model for visual-object-based attention and eye movements. Comput Vis Image Underst. 2008; 112(2):126–42.
25. Zelinsky GJ. A theory of eye movements during target acquisition. Psychol Rev. 2008;115(4):787–835.
26. Koch C, Ullman S. Shifts in selective visual-attention: towards the underlying neural circuitry. Hum Neurobiol. 1985;4(4): 219–27.
27. Treisman AM, Gelade G. Feature-integration theory of attention. Cogn Psychol. 1980;12(1):97–136.
28. Itti L. A saliency-based search mechanism for overt and covert shifts of visual attention. Vision Res. 2000;40:1489–506.
29. Foulsham T, Underwood G How does the purpose of inspection influence the potency of visual salience in scene perception? 2007.
30. Einhauser W, Spain M, Perona P. Objects predict fixations better than early saliency. J Vis. 2008;8(14):11–26.
31. Chen X, Zelinsky GJ. Real-world visual search is dominated by top-down guidance. Vision Res. 2006;46(24):4118–33.
32. Foulsham T, Underwood G. Can the purpose of inspection influence the potency of visual salience in scene perception? Perception. 2006;35:236.
33. Foulsham T, Underwood G. What can saliency models predict about eye movements? Spatial and sequential aspects of fixations during encoding and recognition. J Vis. 2008;8(2).
34. Henderson JM, Malcolm GL, Schandl C. Searching in the dark: cognitive relevance drives attention in real-world scenes. Psychon Bull Rev. 2009;16:850–6.
35. Henderson JM, et al. Eye movements and picture processing during recognition. Percept Psychophys. 2003;65(5):725–34.
36. Hayhoe M, Land M. Coordination of eye and hand movements in a normal visual environment. Invest Ophthalmol Vis Sci. 1999;40(4):S380.
37. Land MF, Hayhoe M. In what ways do eye movements contribute to everyday activities? Vision Res. 2001;41(25–26): 3559–65.
38. Land MF, Lee DN. Where we look when we steer. Nature. 1994;369(6483):742–4.
39. Land MF, McLeod P. From eye movements to actions: how batsmen hit the ball. Nat Neurosci. 2000;3(12):1340–5.
40. Yantis S. Control of visual attention. In: Pashler H, editor. Attention. London: Psychology Press; 1998. p. 223–56.
41. Yantis S, Hillstrom AP. Stimulus-driven attentional capture: evidence from equiluminant visual objects. J Exp Psychol Hum Percept Perform. 1994;20(1):95–107.
42. Yantis S, Jonides J. Abrupt visual onsets and selective attention: evidence from visual search. J Exp Psychol Hum Percept Perform. 1984;10(5):601–21.
43. Brockmole JR, Henderson JM. Prioritization of new objects in real-world scenes: evidence from eye movements. J Exp Psychol Hum Percept Perform. 2005;31(5):857–68.
44. Brockmole JR, Henderson JM. Object appearance disappearance, and attention prioritization in real-world scenes. Psychon Bull Rev. 2005;12(6):1061–7.
45. Matsukura M, Brockmole JR, Henderson JM. Overt attentional prioritization of new objects and feature changes during real-world scene viewing. Vis Cogn. 2009;6(7):835–55.
46. Simons DJ. Attentional capture and inattentional blindness. Trends Cogn Sci. 2000;4(4):147–55.
47. Berg DJ, et al. Free viewing of dynamic stimuli by humans and monkeys. J Vis. 2009;9(5):1–15.
48. Carmi R, Itti L. Visual causes versus correlates of attentional selection in dynamic scenes. Vision Res. 2006;46(26):4333–45.
49. Carmi R, Itti L. The role of memory in guiding attention during natural vision. J Vis. 2006;6(9):898–914.

50. Itti L. Quantifying the contribution of low-level saliency to human eye movements in dynamic scenes. Vis Cogn. 2005; 12(6):1093–123.
51. Itti L. Quantitative modelling of perceptual salience at human eye position. Vis Cogn. 2006;14(4–8):959–84.
52. Le Meur O, Le Callet P, Barba D. Predicting visual fixations on video based on low-level visual features. Vision Res. 2007;47(19):2483–98.
53. t'Hart BM, et al. Gaze allocation in natural stimuli: comparing free exploration to head-fixed viewing conditions. Vis Cogn. 2009;17(6/7):1132–58.
54. Goldstein RB, Woods RL, Peli E. Where people look when watching movies: do all viewers look at the same place? Comput Biol Med. 2007;37(7):957–64.
55. Hasson U, et al. Neurocinematics: the Neuroscience of Film. Proje J Movies Mind. 2008;2(1):1–26.
56. Marchant P, et al. Are you seeing what i'm seeing? an eye-tracking evaluation of dynamic scenes. Digit Creat. 2009;20(3): 153–63.
57. May J, Dean MP, Barnard PJ. Using film cutting techniques in interface design. Hum Comput Interact. 2003;18:325–72.
58. Nyström M, Holmqvist K. Effect of compressed offline foveated video on viewing behavior and subjective quality. ACM Transon Multimed Comput Commun Appl. 2010;6(1):1–16.
59. Sawahata Y, et al. Determining comprehension and quality of tv programs using eye-gaze tracking. Pattern Recognit. 2008;41(5): 1610–26.
60. Smith TJ, Henderson JM. Attentional synchrony in static and dynamic scenes. J Vis. 2008;8(6):773.
61. Stelmach LB, Tam WJ, Hearty PJ. Static and dynamic spatial resolution in image coding: an investigation of eye movements. In human vision, visual processing, and digital display II. 1991.
62. Tosi V, Mecacci L, Pasquali E. Pasquali, scanning eye movements made when viewing film: preliminary observations. Int J Neurosci. 1997;92(1/2):47–52.
63. Smith TJ. An attentional theory of continuity editing, in informatics. Edinburgh, UK: University of Edinburgh; 2006. p. 400.
64. Cristino F, Baddeley R. The nature of the visual representations involved in eye movements when walking down the street. Vis cogn. 2009;17(6–7):880–903.
65. Tatler BW. The central fixation bias in scene viewing: selecting an optimal viewing position independently of motor biases and image feature distributions. J Vis. 2007;7(14):1–17.
66. Tseng PH, et al. Quantifying centre bias of observers in free viewing of dynamic natural scenes. J Vis. 2009;9(7):1–16.
67. Torralba A, Oliva A. Statistics of natural image categories. Netw-Comput Neural Syst. 2003;14(3):391–412.
68. Palmer SE. Vision Science: photons to phenomenology. Cambridge, Mass: London MIT Press; 1999. Xxii. p. 810. ill. 26 cm.
69. Murphy BJ. Pattern thresholds for moving and stationary gratings during smooth eye movement. Vision Res. 1978;18(5):521–30.
70. Carandini M, Heeger DJ. Summation and division by neurons in primate visual cortex. Science. 1994;264(5163):1333–6.
71. Itti L, Koch C, Niebur E. A model of saliency-based visual attention for rapid scene analysis. IEEE Trans Pattern Anal Mach Intell. 1998;20(11):1254–9.
72. Bex PJ, Makous W. Spatial frequency, phase, and the contrast of natural images. J Opt Soc Am A Opt Image Sci Vis. 2002;19(6):1096–106.
73. Moulden B, Kingdom F, Gatley LF. The standard-deviation of luminance as a metric for contrast in random-dot images. Perception. 1990;19(1):79–101.
74. Lee DK, et al. Attention activates winner-take-all competition among visual filters. Nat Neurosci. 1999;2(4):375–81.
75. Rosenholtz R. A simple saliency model predicts a number of motion popout phenomena. Vision Res. 1999;39(19):3157–63.
76. Einhauser W, Konig P. Does luminance-contrast contribute to a saliency map for overt visual attention? Eur J Neurosci. 2003;17(5):1089–97.
77. Itti L, Baldi P. A principled approach to detecting surprising events in video. In: SchmidC, Soatto S, Tomasi C, editors. 2005 IEEE computer society conference on computer vision and pattern recognition, Vol 1, proceedings. Los Alamitos: Ieee Computer Soc; 2005. p. 631–37.
78. Rosin PL. A simple method for detecting salient regions. Pattern Recognit. 2009;42(11):2363–71.
79. Park SJ, Shin JK, Lee M. Biologically inspired saliency map model for bottom-up visual attention. In: Bulthoff HH et al., editors. Biologically motivated computer vision, proceedings. Berlin: Springer; 2002. p. 418-426.
80. Privitera CM, Stark LW. Human-vision-based selection of image processing algorithms for planetary exploration. IEEE Trans Image Process. 2003;12(8):917–23.
81. Sobel I, Feldman G. A 3×3 isotropic gradient operator for image processing; presented talk at the Stanford Artificial Project 1968. In: Duda RO, Hart PE, editors. Pattern classification and scene analysis. New York: Wiley; 1973. p. 271–2.
82. Attneave F. Some informational aspects of visual perception. Psychol Rev. 1954;61(3):183–93.
83. Schmid C, Mohr R, Bauckhage C. Evaluation of interest point detectors. Int J Comput Vis. 2000;37(2):151–72.
84. Noble JA. Finding corners. Image Vis Comput. 1988;6(2): 121–8.
85. Moravec HP. Obstacle avoidance and navigation in the real world by a seeing robot rover, in Robotics Institute, Carnegie Mellon University & doctoral dissertation, Stanford University. 1980.
86. Harris C, Stephens M. A combined corner and edge detector. in 4th Alvey Vision Conference. Manchester; 1988.
87. Blakemore C, Campbell FW. On existence of neurones in human visual system selectively sensitive to orientation and size of retinal images. J Physiol. 1969;203(1):237–60.
88. Hubel DH, Wiesel TN. Receptive fields, binocular interaction and functional architecture in the cat's visual cortex. J Physiol. 1962;160(1):106–54.
89. Field DJ. Relations between the statistics of natural images and the response properties of cortical-cells. J Opt Soc Am A Opt Image Sci Vis. 1987;4(12):2379–94.
90. Anstis SM. Apparent movement. In: Held RH, Leibowitz W, Teuber H-L, editors. Handbook of sensory physiology. New York: Springer; 1977.
91. Anstis SM, Mackay DM. The perception of apparent movement. Philos Trans R Soc Lond B Biol Sci. 1980;290(1038):153–68.
92. Ullman, S., The interpretation of visual motion. The MIT Press Series in Artificial Intelligence. Cambridge, Mass: M.I.T. Press; 1979. Xiii. p. 229. ill. 24 cm.
93. Adelson EH, Bergen JR. Spatiotemporal energy models for the perception of motion. J Opt Soc Am A Opt Image Sci Vis. 1985;2(2):284–99.
94. Theeuwes J. Abrupt luminance change pops out; abrupt color change does not. Percept Psychophys. 1995;57(5):637–44.
95. Moulden B, Renshaw J, Mather G. 2 channels for flicker in the human visual-system. Perception. 1984;13(4):387–400.
96. Horn BKP, Schunck BG. Determining optical flow. Artif Intell. 1981;17(1–3):185–203.
97. Lucas BD, Kanade T. An iterative image registration technique with an application to stereo vision. In Proceedings of the DARPA imaging understanding workshop. 1981. p. 121–130.
98. Baddeley R. Searching for filters with 'interesting' output distributions: an uninteresting direction to explore? Netw-Comput Neural Syst. 1996;7(2):409–21.

99. Green DM, Swets JA. Signal detection theory and psychophysics. New York: Wiley: 1966. Xi. p. 455. illus24 cm.
100. Privitera CM, Stark LW. Algorithms for defining visual regions-of-interest: comparison with eye fixations. IEEE Trans Pattern Anal Mach Intell. 2000;22(9):970–82.
101. Latimer CR. Eye-movement data: cumulative fixation time and cluster-analysis. Behav Res Methods Instrum Comput. 1988; 20(5):437–70.
102. Santella A, DeCarlo D. Robust clustering of eye movement recordings for quantification of visual interest. In eye tracking research & application. San Antonio, Texas: ACM Press; 2004.
103. Bishop, C.M., Pattern recognition and machine learning. Information science and statistics. New York: Springer; 2006. xx. p. 738.
104. Torre V, Poggio T. On edge detection. IEEE Trans Pattern Anal Mach Intell. 1984;8(2):147–63.
105. Mannan SK, Ruddock KH, Wooding DS. The relationship between the locations of spatial features and those of fixations made during visual examination of briefly presented images. Spat Vis. 1996;10:165–88.
106. Mannan SK, Ruddock KH, Wooding DS. Fixation sequences made during visual examination of briefly presented 2D images. Spat Vis. 1997;11:157–78.
107. Torralba A, et al. Contextual guidance of eye movements and attention in real-world scenes: the role of global features in object search. Psychol Rev. 2006;113(4):766–86.
108. Vincent BT, et al. Do we look at lights? Using mixture modelling to distinguish between low- and high-level factors in natural image viewing. Vis Cogn. 2009;17(6/7):856–79.
109. Zacks JM, et al. Human brain activity time-locked to perceptual event boundaries. Nat Neurosci. 2001;4:651–5.
110. Speer NK, Swallow KM, Zacks JM. Activation of human motion processing areas during event perception. Cogn Affect Behav Neurosci. 2003;3:335–45.
111. Zacks JM, et al. Visual motion and the neural correlates of event perception. Brain Res. 2006;1076:150–62.
112. Bordwell D, Thompson K. Film art: an introduction, vol. 6. USA: McGraw Hill; 2001.
113. Nyström M, Holmqvist K. Variable resolution images and their effects on eye movements during free-viewing. In human vision and electronic imaging XII. San Jose, CA; 2007.
114. Nyström M, Holmqvist K. Semantic override of low-level features in image viewing: both initially and overall. J Eye Mov Res. 2008;2(2):1–11.
115. Frank MC, Vul E, Johnson SP. Development of infants' attention to faces during the first year. Cognition. 2009;110:160–70.